

# Cs deposition on *c*-axis-oriented thin films of $\alpha$ -(BEDT-TTF) $_2$ I $_3$ : evidence for electron doping and intercalation

S. Söderholm<sup>a</sup>, B. Loppinet<sup>a</sup>, D. Schweitzer<sup>b</sup>

<sup>a</sup>Materials Physics, Department of Physics, Royal Institute of Technology, S-100 44 Stockholm, Sweden

<sup>b</sup>3. Physikalisches Institut, Universität Stuttgart, Pfaffenwaldring 57, D-70550 Stuttgart, Germany

Received 15 January 1994; accepted 21 February 1994

## Abstract

The deposition of Cs on *c*-axis-oriented thin films of  $\alpha$ -(BEDT-TTF) $_2$ I $_3$  causes a shift of the chemical potential in agreement with addition of electrons to the system. At high Cs doses a chemical reaction between Cs<sup>+</sup> and I $_3$ <sup>−</sup> occurs, with the formation of CsI and probably mainly I $_2$ . In the valence-band regime new structures appear, due to I $_2$ , i.e., CsI, and molecular orbitals of I $_2$  derived from I 5p. The hybridization between these orbitals and the BEDT-TTF orbitals is negligible. The remarkable changes in the I 4d spectrum caused by Cs deposition can be understood within the framework of the proposed chemical reaction.

**Keywords:** Cesium; Doping; Intercalation; Superconductors

## 1. Introduction

Since the synthesis of the first sulfur-containing ambient-pressure organic superconductor,  $\beta$ -(BEDT-TTF) $_2$ I $_3$ , where BEDT-TTF is an abbreviation for bis(ethylenedithio)-tetrathiafulvalene, in 1983 [1], much effort has been spent on studies of charge-transfer complexes (CT complexes) based on BEDT-TTF. There are several reasons for this; among them, that most of the organic superconductors known today are based on BEDT-TTF, and organic conductors of BEDT-TTF appear in many crystallographic phases and have widely different properties. However, the BEDT-TTF salts generally have a layered structure consisting of alternating layers of conducting BEDT-TTF molecules and of anions. These facts make this class of materials well suited for studies of fundamental questions, i.e., the relation between crystal structure and electronic properties, the mechanism behind superconductivity, the importance of electron–electron interaction, etc.

Photoemission experiments may provide important information about the electronic structure, and if a perturbation is applied, i.e., an adsorbate/overlayer, additional information about the electronic system can be obtained.

In this communication a photoemission study of the interaction between *c*-axis-oriented thin films of  $\alpha$ -(BEDT-TTF) $_2$ I $_3$  and Cs is reported. The purpose of the experiment was to study how the addition of electrons to  $\alpha$ -(BEDT-TTF) $_2$ I $_3$ , a hole conductor [2], influences the electronic structure of the CT complex and thereby to gain more knowledge about  $\alpha$ -(BEDT-TTF) $_2$ I $_3$ . Cs was chosen as the electron donor because of its low electronegativity and large ionic radius, in comparison with other alkali metals, in order to have a lower probability of diffusion of the dopant into the films. Cs was chosen for these reasons, in spite of the risk of a chemical reaction occurring between iodine and Cs at high doses of Cs.

## 2. Experimental

The photoemission experiments were performed at beamline 41 at the MAX synchrotron radiation laboratory in Lund, Sweden. The spectra were recorded with a goniometer-mounted modified VSW hemispherical angle resolving electron energy analyser; for a comprehensive description of the beamline see Karlsson et al. [3]. The total energy resolution, photon and electron contributions, was determined from the Fermi

edge of thoroughly sputtered Au and stainless steel to be 0.3 eV at a photon energy of 100 eV. The latter was used as a reference for the  $\alpha$ -(BEDT-TTF)<sub>2</sub>I<sub>3</sub> spectra recorded. The synchrotron radiation angle of incidence was 45°, in order to probe electron states parallel and perpendicular to the surface with the same probability. The base pressure in the analysis chamber was less than  $5 \times 10^{-10}$  mbar.

The *c*-axis-oriented thin films of  $\alpha$ -(BEDT-TTF)<sub>2</sub>I<sub>3</sub> were prepared by physical vapour deposition (PVD), essentially according to the method of Kawabata et al. [4], in a custom-made preparation chamber attached to the analysis chamber on the beamline. A comprehensive description of the film preparation and the equipment is given in Ref. [5]. X-ray diffraction showed that the films are *c*-axis oriented, with the *c*-axis perpendicular to the substrate, and approximately 45% of the crystallites are oriented within 5°. Scanning electron microscopy (SEM) images showed that the crystallites are roughly 1–2  $\mu$ m large and that a *c*-axis orientation is preferred [5].

Cs was deposited from a SAES getter source, and the amount of deposited Cs was monitored through the change in the work function, i.e., the cut-off of the secondary electrons. These measurements were performed immediately after the Cs deposition and after the photoemission spectra had been recorded at that particular coverage.

### 3. Results and discussion

The measurements of the change in the work function,  $\Delta\Phi$ , showed that it decreased during the recording of the photoemission spectra at a particular Cs coverage (see Table 1). Since the valence-band regime was recorded immediately after the first measurement,  $\Delta\Phi_B$ , that value of the work function change will be used in connection with the valence-band spectra, and the second value,  $\Delta\Phi_A$ , in connection with the I 4d core-level spectra, since it was determined immediately after recording the I 4d level.  $\Delta\Phi_A$  was measured about 2 h after  $\Delta\Phi_B$  was measured. The width of the cut-off, measured between 10 and 90% of the height of the cut-off edge, was the same for the clean surface and for the spectra corresponding to the work function

measurements for the shortest Cs deposition, the width being 0.21 eV. Additional Cs deposition caused the width to increase slowly to 0.37 eV. For the highest coverages, the width corresponding to  $\Delta\Phi_A$  was slightly larger than the width corresponding to  $\Delta\Phi_B$ . No signs of structure around the cut-off energy were detected in any spectra. The maximum amount of deposited Cs is estimated to be of the order of one monolayer.

At small amounts of deposited Cs, as in the present case, the Cs coverage can be regarded as an array of ions. The ionic character of the deposited Cs causes a decrease in the work function through the formation of a dipole layer in the surface, consisting of the charged adatoms and their images. Thus the change in the work function when Cs is deposited indicates that a charge transfer from Cs to  $\alpha$ -(BEDT-TTF)<sub>2</sub>I<sub>3</sub> occurs. The decrease in the change in the work function with time is due to diffusion of Cs into the  $\alpha$ -(BEDT-TTF)<sub>2</sub>I<sub>3</sub> and not to desorption, since the intensity of the Cs 5p core level increases after each deposition, even if the measured  $\Delta\Phi_B$  value is the same, and  $\Delta\Phi_A$  is almost the same (see the spectra normalized to the photon flux in Fig. 1, in particular spectra c and d).

In the valence-band regime of clean  $\alpha$ -(BEDT-TTF)<sub>2</sub>I<sub>3</sub> (Fig. 1(a)) five distinct structures are seen. (The spectrum of the clean film is discussed in Ref. [5].) Upon Cs deposition, these structures shift to higher binding energies  $E_b$  with respect to the Fermi level  $E_F$  and additional peaks appear: the Cs 5p<sub>1/2</sub> and 5p<sub>3/2</sub> peaks and three structures with  $E_b$  between 3 and 8 eV. The latter structures are seen only at the highest Cs doses (see Fig. 1). The binding energy of the Cs 5p<sub>3/2</sub> peak is 10.5 eV at the highest Cs doses. Scans over an extended binding energy range did not reveal any other Cs 5p peaks.

The I 4d spectrum is drastically altered by Cs deposition; compare spectra a and d in Fig. 2. The spectrum of the clean surface can be fitted well by one doublet with  $E_b(5/2) = 48.9$  eV and a spin-orbit split of 1.71 eV. The fitted lineshape was obtained through a convolution of a Lorentzian line with a Gaussian line with full widths at half maximum (FWHM) of 0.20 and 0.92 eV, respectively. The Gaussian line simulates broadening of the spectrum due to the resolution of the apparatus, phonons and disorder, and the Lorentzian line the lifetime of the core hole. Already after the first deposition a new component appears at higher binding energies. After further Cs deposition, additional I 4d peaks appear and the total intensity increases. In order to simulate spectra c and d in Fig. 2, four Cs-induced doublets must be used, with a Gaussian FWHM of 1.6 eV. The branching ratio of the intrinsic doublet is changed from 1.33 to 1.6 as soon as Cs is deposited; this ratio is also used for peaks 2 and 5, but a ratio of 2 must be used for peaks 3 and 4. The simulation performed showed that the binding energy of the in-

Table 1  
Measured change in the work function  $\Delta\Phi$  before and after the photoelectron spectroscopy (PES) experiments

Deposition no. (min)	$\Delta\Phi$ before PES	$\Delta\Phi$ after PES	Spectrum in Figs. 1 and 2
1 (1)	−0.26	−0.06	b
2 (3)	−0.79	−0.32	c
3 (3)	−0.79	−0.39	d



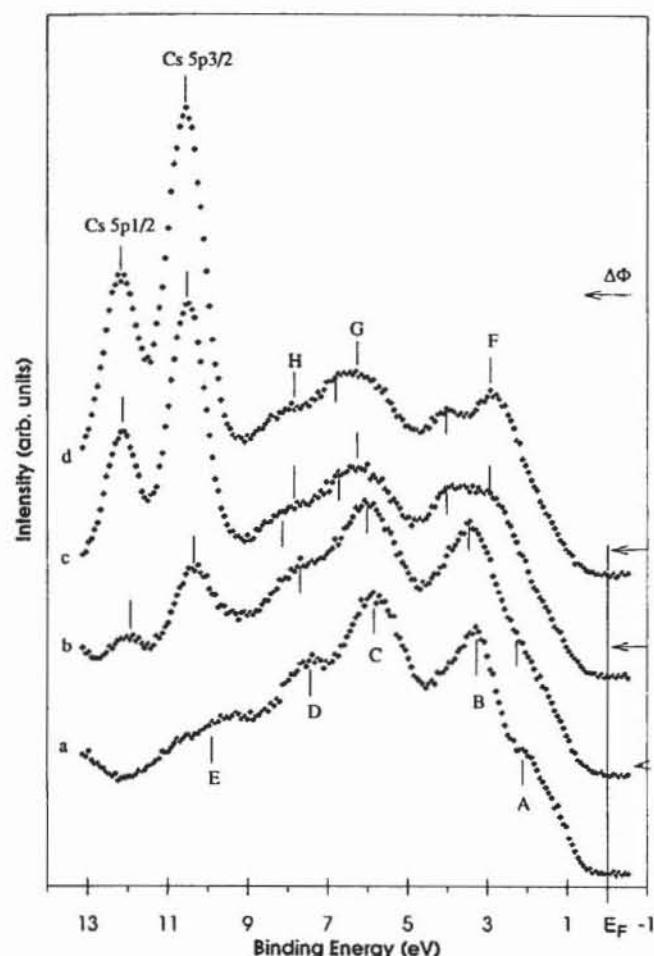


Fig. 1. Photoemission spectra of an  $\alpha$ -(BEDT-TTF) $_2$ I $_3$  film obtained in normal emission with a photon energy of 100 eV, showing the valence-band regime after the deposition of various amounts of Cs. Labels A–E and the corresponding bars below the spectra indicate different structures present in the clean film. Structures associated with the deposition of Cs are labelled F–H and indicated with bars above the spectra. The Cs 5p peaks are also indicated. Spectrum a is of the clean surface, b corresponds to a work function change of  $\Delta\Phi_B = -0.26$  eV, c to  $\Delta\Phi_B = -0.79$  eV, and d to  $\Delta\Phi_B = -0.79$  eV.

intrinsic I 4d is shifted towards higher binding energy when Cs is deposited. This shift can be ascribed to a shift of the chemical potential, not to a chemical shift, since the energy difference between this core level and the valence-band features (A–E) is not changed by the Cs deposition. The Cs-induced I 4d peaks are shifted by 6.5, 3.6, 1.0 and  $-1.0$  eV at the highest Cs dose, with respect to the intrinsic I 4d peak.

The simulation presented is not unique; the parameters were chosen so that they remained constant for all Cs coverages and so that as few as possible changed with respect to the clean surface, and the number of peaks was kept as low as possible. The change in branching ratio is justified by the rapid variation of the cross section for I 4d in the photon energy range used [6] and the simultaneous variation of the branching ratio [7], together with diffraction effects caused by the presence of an overlayer. The change in the linewidth is discussed below.

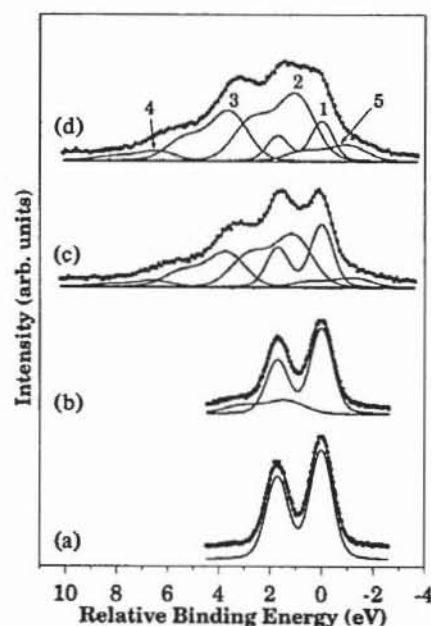


Fig. 2. I 4d core-level spectra, excited with a photon energy of 100 eV, after deposition of various amounts of Cs. Spectrum a is of the clean surface, b corresponds to a work function change of  $\Delta\Phi_A = -0.06$  eV, c to  $\Delta\Phi_A = -0.32$  eV, and d to  $\Delta\Phi_A = -0.39$  eV. Solid lines are the results of simulations; the parameters used in the simulations are given in the text. The binding energy scale is relative to the binding energy of the 4d $_{5/2}$  level present before deposition of Cs. The Cs deposition causes the binding energy with respect to  $E_F$  to increase by an amount equal to  $\Delta\Phi_A$ .

Structures A–E, which arise from  $\alpha$ -(BEDT-TTF) $_2$ I $_3$ , all show the same energy shift towards higher binding energy after the deposition of Cs (see Fig. 1). This rigid shift of the valence band can be ascribed to a shift of the chemical potential due to the addition of electrons to the system through the deposition of Cs. The apparent shift of the Fermi level with respect to the valence-band features is in agreement with addition of electrons to the organic conductor, due to a charge transfer from the deposited Cs. Furthermore, the valence-band maximum is found at the same binding energy after the deposition of Cs, although structures A–E are shifted towards higher binding energy, which indicates that additional states become occupied through the Cs deposition, i.e., electron doping occurs.

Even in the spectrum corresponding to the highest Cs doses, structures B, C and D are recognizable and have the same energy separation. The same probably holds for structures A and E, which are obscured by Cs-induced structure F and the Cs 5p $_{5/2}$  peak, respectively. This implies that the molecular orbitals forming the valence band are unaffected by the Cs deposition and that the hybridization between the Cs-induced orbitals and the molecular orbitals of BEDT-TTF is negligible, i.e., the bands still represent their molecular identities, as expected for a molecular solid consisting of distinctly different species. In other words, no chemical reaction involving the BEDT-TTF molecules occurs.

The remarkable changes in the I 4d spectrum upon Cs deposition can be explained by a chemical reaction between  $\text{Cs}^+$  and  $\text{I}_3^-$ , since scanning tunnelling microscopy [8,9] and photoelectron spectroscopy [5] indicate that the surface layer consists of BEDT-TTF and Cs, must diffuse into the substrate in order to react with the iodine. In this picture the  $\text{Cs}^+$  ions diffuse into the crystal, and when they encounter the  $\text{I}_3^-$  layer they react with the iodine, and CsI and most likely mainly  $\text{I}_2$  molecules are formed. The production of small amounts of other iodine species such as  $\text{I}^-$  (not involved in forming CsI) and  $\text{I}_5^-$ , and the subsequent formation of complex iodine species, cannot be ruled out. A plot of the intensity of the different I 4d peaks (labelled 1–5 in Fig. 2) as a function of Cs evaporation time reveals that the intensity of peaks 2 and 3 initially increases rapidly, indicating that these iodine species are situated closer to the surface than the  $\text{I}_3^-$  ions. This diffusion explains the increasing intensity of the I 4d spectrum after deposition of Cs.

The binding energy of the Cs-induced peaks cannot be used to make assignments of the different peaks, since  $E_b$  for different iodine-containing compounds varies between 47 and 52 eV [10,11]. The binding energy of the Cs  $5p_{3/2}$  level is lower than that typically found for ionic Cs species (between 11 and 12 eV), for instance on  $\text{Bi}_2\text{Sr}_2\text{CaCu}_2\text{O}_8$  ( $E_b = 11.5$  eV) [12] and as a dopant in the conducting polymer bithiophene ( $E_b = 12$  eV) [13], but the same low binding energy is found for Cs in CsI [14] and for Cs intercalated in the layered metal chalcogenide  $2\text{H TaSe}_2$  [15], supporting the proposed chemical reaction. Neither can the relative intensities of the different Cs-induced iodine species be used in an assignment of these peaks, based on quantitative arguments, since the average distance to the surface for the different Cs-induced iodine species is unknown.

However, based on the assumption that besides CsI mainly  $\text{I}_2$  is formed via the chemical reaction, the following tentative assignments of the Cs-induced I 4d doublets can be made. Peak 2 corresponds to  $\text{I}_2$  formed in the reaction. The peak with the lowest binding energy is due to  $\text{I}^-$ , i.e., CsI, which is more reduced than  $\text{I}_3^-$ , causing the binding energy to shift to lower energy. The low intensity of this peak in comparison with the  $\text{I}_2$  peak (and peak 3) suggests that the CsI stays in the  $\text{I}_3^-$  layer. The assignment of peaks 3 and 4 is more uncertain. There exist several possibilities: if mainly  $\text{I}_2$  is formed, 3 could correspond to  $\text{I}_2$  in different surroundings and 4 could be due to the other iodine species, or both 3 and 4 could be due to  $\text{I}_2$ , or both 3 and 4 could correspond to other iodine species, etc. The rather large Gaussian FWHM needed for peaks 2–5 in the fits is attributed to disorder, i.e., the iodine species formed in the reaction with  $\text{Cs}^+$  have a random spatial distribution, and some or all of these peaks could very well consist of unresolved components. This

contribution is added to the contribution from molecular vibrations, which is fairly large from the beginning, as evident from the Gaussian FWHM of the clean film, 0.92 eV.

Since structures F–H, appearing in the valence-band regime as a consequence of Cs deposition, become discernible at the same Cs dose that drastically alters the I 4d spectrum, these structures can be attributed to CsI and  $\text{I}_2$ . Thus, structure F is assigned to the 5p level of  $\text{I}^-$  in CsI, which forms a band with  $E_b = 3$ –4 eV [14], and G and H to molecular orbitals formed by the 5p orbitals of iodine atoms having binding energies in the range 5–11 eV in solid  $\text{I}_2$  [16]. The broadness of structure G indicates that it consists of unresolved components.

In summary, the deposition of Cs causes a shift of the chemical potential in agreement with the addition of electrons to the system. In the valence-band regime new structures appear that can be attributed to  $\text{I}^-$ , i.e., CsI, and molecular orbitals of  $\text{I}_2$  derived from I 5p. The presence of these species is the result of a chemical reaction in which  $\text{Cs}^+$  and  $\text{I}_3^-$  react and CsI and mainly  $\text{I}_2$  are formed. The Cs-induced structures are superimposed on an unaltered valence band, indicating that the hybridization between the BEDT-TTF orbitals forming the valence band and the Cs-induced iodine orbitals is small.

The chemical reaction gives rise to remarkable changes in the I 4d spectrum. A simulation shows that four I 4d doublets appear as a consequence of the Cs deposition. These peaks can tentatively be assigned within the framework of the proposed chemical reaction.

## Acknowledgements

Financial support from the Göran Gustafssons Foundation and the Swedish Natural Science Research Council is gratefully acknowledged.

## References

- [1] E.B. Yagubskii, I.F. Shchegolev, V.N. Laukhin, P.A. Kononovich, M.V. Kartsovnic, A.V. Zvarykina and L.I. Bubarov, *JETP Lett.*, 39 (1984) 12.
- [2] K. Bender, I. Hennig, D. Schweitzer, K. Dietz, H. Endres and H.J. Keller, *Mol. Cryst. Liq. Cryst.*, 107 (1984) 359; I. Hennig, K. Bender, D. Schweitzer, K. Dietz, H. Endres, H.J. Keller, A. Gleitz and H.W. Helberg, *Mol. Cryst. Liq. Cryst.*, 119 (1985) 337.
- [3] U.O. Karlsson, J.N. Andersen, K. Hansen and R. Nyholm, *Nucl. Instrum. Methods A*, 282 (1989) 553.
- [4] K. Kawabata, K. Tanaka and M. Mizutani, *Solid State Commun.*, 74 (1990) 83; K. Kawabata, K. Tanaka and M. Mizutani, *Synth. Met.*, 41–43 (1991) 2097.
- [5] S. Söderholm, B. Loppinet and D. Schweitzer, *Synth. Met.*, 62 (1994) 187.

- [6] J.J. Yeh and I. Lindau, *At. Data Nucl. Data Tables*, 32 (1985) 1.
- [7] L.I. Johansson, I. Lindau, M.H. Hecht and E. Källne, *Solid State Commun.*, 34 (1980) 83.
- [8] Y.F. Miura, A. Kasai, T. Nakamura, H. Komizu, M. Matsumoto and Y. Kawabata, *Mol. Cryst. Liq. Cryst.*, 196 (1991) 161.
- [9] M. Yoshimura, H. Shigekawa, H. Yamochi, G. Saito, Y. Saito and A. Kawazu, *Phys. Rev. B*, 44 (1991) 1970.
- [10] S. Host, D.F. van de Vondel and G.P. van der Kelen, *J. Electron Spectrosc. Relat. Phenom.*, 17 (1979) 191.
- [11] P.M.Th.M. van Attekum, J.W.A. van der Velden and J.M. Trooster, *Inorg. Chem.*, 19 (1980) 701.
- [12] S. Söderholm, M. Qvarford, H. Bernhoff, J.N. Andersen, E. Lundgren, R. Nyholm, U.O. Karlsson, I. Lindau and S.A. Flodström, to be published.
- [13] D. Steinmüller, M.G. Ramsey and F.P. Netzer, *Phys. Rev. B*, 47 (1993) 13 323.
- [14] T.H. DiStefano and W.E. Spicer, *Phys. Rev. B*, 7 (1973) 1554.
- [15] C. Pettenkofer, W. Jaegermann, A. Schellenberger, E. Holub-Krappe, C.A. Papageorgopoulos, M. Karamatos and A. Papageorgopoulos, *Solid State Commun.*, 84 (1992) 921.
- [16] H. Yamamoto, K. Seki, T. Mori and H. Inokuchi, *J. Chem. Phys.*, 86 (1987) 1775.